

## Enhancement of tetracene photovoltaic devices with heat treatment

Yan Shao, Srinivas Sista, Chih-Wei Chu, Douglas Sievers, and Yang Yang<sup>a)</sup>  
 Department of Materials Science and Engineering, University of California-Los Angeles,  
 Los Angeles, California 90095

(Received 9 October 2006; accepted 23 January 2007; published online 5 March 2007)

An efficient photovoltaic heterojunction of tetracene and fullerene has been investigated, and high performance organic solar cells have been demonstrated by thermal deposition and successive heat treatment. After the heat treatment, the open circuit voltage of the devices was enhanced greatly and at the same time the photocurrent remained almost unchanged. The series resistance of the devices was reduced and the fill factor was slightly enhanced. Consequently, the power conversion efficiency was improved from 1.7% to 2.2%. The preliminary conclusion for this enhancement is due to the part crystallization of the tetracene layer and consequent morphological change, which were supported by atomic force microscopy images, absorption spectra, and x-ray diffraction analysis. The part crystallization results in increase in hole mobility as evidenced by hole mobility measurements. © 2007 American Institute of Physics. [DOI: 10.1063/1.2709505]

Important progress has been made for organic photovoltaic cells since the donor and acceptor heterojunction structure was introduced in 1986.<sup>1</sup> A number of organic semiconductors including both conjugated polymers and small molecules have been investigated and the power conversion efficiencies of the photovoltaic device have improved steadily.<sup>2-4</sup> Some organic materials have been identified as potential candidates for photovoltaic application, which include poly(3-hexylthiophene) (P3HT),<sup>4</sup> methanofullerene [6,6]-phenyl C<sub>61</sub> butyric acid methyl ester (PCBM),<sup>5</sup> copper phthalocyanine (CuPc),<sup>6</sup> buckminsterfullerene (C<sub>60</sub>),<sup>7</sup> poly(2-methoxy-5-(2'-ethyl-hexyloxy)-1,4-phenylene vinylene),<sup>8</sup> pentacene,<sup>9,10</sup> and tetracene.<sup>11</sup>

Organic materials with high mobilities are desired for high efficiency photovoltaic device fabrication. Recently, tetracene and its derivatives<sup>12-15</sup> have been investigated extensively for fabricating light-emitting transistors<sup>13,15</sup> and field effect transistors,<sup>14</sup> since they possess relatively high hole mobilities on the order of 0.1 cm<sup>2</sup> V<sup>-1</sup> s<sup>-1</sup> in the single crystal or microcrystal states.<sup>12</sup> The high mobility of tetracene can also be utilized to extend the exciton diffusion length in organic solar cells and a relatively thick donor layer can be formed in order to enhance light absorption. The highest occupied molecular orbital of tetracene is about 5.4 eV,<sup>11</sup> which matches well with the work function of the traditional indium tin oxide (ITO) electrode with a poly(3,4-ethylenedioxythiophene):poly(styrene sulfonate) (PEDOT:PSS) coating layer. When the classic acceptor material C<sub>60</sub> is adopted, an efficient photovoltaic heterojunction structure can be formed with proper energy level offset.

The tetracene/C<sub>60</sub> photovoltaic devices were fabricated on patterned ITO-coated glass substrates, which had been carefully cleaned by successive ultrasonic treatment in acetone and isopropyl alcohol. After the cleaned ITO glass was subject to UV-ozone treatment, a thin layer of PEDOT:PSS film was spin coated onto the ITO glass with a speed of 4000 rpm for about 1 min and then baked at 115 °C for 50 min in ambient. The fabrication process was conducted in

a thermal vapor deposition chamber with a base pressure of  $\sim 1.3 \times 10^{-6}$  Torr and the evaporation rates for tetracene, C<sub>60</sub>, BCP, and Al were  $\sim 0.2$ – $0.3$ ,  $\sim 0.9$ ,  $\sim 0.6$ , and  $\sim 7$  Å/s, respectively. All the organic materials used in the device fabrication were used as received without further purification. The active area of the device defined by shadow mask is  $\sim 0.11$  cm<sup>2</sup>. The photocurrent was measured under AM1.5 solar illumination at 130 mW/cm<sup>2</sup> (1.3 sun) supplied by a ThermalOriel of 150 W solar simulator with AM1.5G filter set and the light intensity was determined by a monosilicon detector (with KG-5 visible color filter) calibrated by National Renewable Energy Laboratory (NREL) to minimize spectral mismatch. All efficiency values reported in this work have been corrected with the spectral mismatch factor.<sup>16</sup>

Figure 1(a) shows the chemical structures of all the organic materials used, a schematic diagram of the photovoltaic device structure, and the current density–voltage (*I*-*V*) curves in the dark (dash dot line) and under 130 mW/cm<sup>2</sup> AM1.5G illumination (solid line) for the photovoltaic device with the structure ITO/PEDOT/tetracene(1000 Å)/C<sub>60</sub>(300 Å)/BCP(80 Å)/Al(1000 Å). The series resistance (*R*<sub>s</sub>) can be calculated from the nearly linear part of the dark current curve and was found to be about 11.3 Ω cm<sup>2</sup> for devices consisting of 1000 Å tetracene and 300 Å C<sub>60</sub>. Here the relatively thick tetracene film did not result in a very large *R*<sub>s</sub>, which reflects the high hole mobility of this molecule. The open circuit voltage (*V*<sub>OC</sub>) is 0.58 V, the short circuit current density (*I*<sub>SC</sub>) is 6.9 mA/cm<sup>2</sup>, and the fill factor is 0.55, which gives a power conversion efficiency of 1.7%. Figure 1(b) shows the dark current (dash dot line) and photocurrent (solid line) density–voltage (*I*-*V*) curves of the photovoltaic device with the same structure after 30 min heat treatment at 100 °C in a glove box under nitrogen environment. The inset diagram shows the calculation of *R*<sub>s</sub> of the heated device from the linear part of the dark curve, which is about 8.7 Ω cm<sup>2</sup>. It can be observed from this diagram that the *V*<sub>OC</sub> has been enhanced greatly to 0.67 V, the fill factor to 0.61, and the *I*<sub>SC</sub> is 6.85 mA/cm<sup>2</sup>, which is almost unchanged. Consequently, the energy conversion efficiency has been improved to 2.2%.

<sup>a)</sup> Author to whom correspondence should be addressed; electronic mail: yangy@ucla.edu

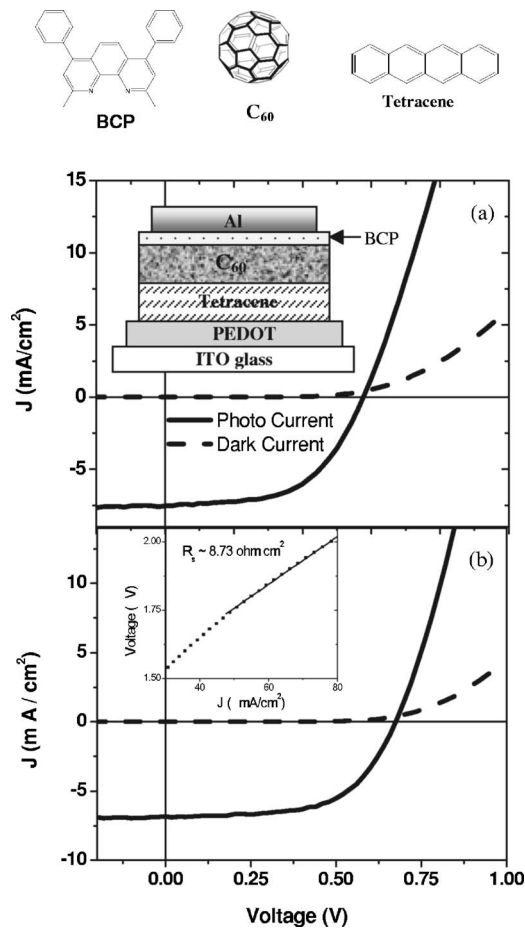


FIG. 1. (a) Chemical structures of the used organic materials, a schematic diagram of the photovoltaic device structure, and the current density–voltage ( $I$ - $V$ ) curves in dark (dash dot line) and under  $130 \text{ mW/cm}^2$  AM1.5G illumination (solid line) of the photovoltaic device with the structure ITO/PEDOT/tetracene( $1000 \text{ \AA}$ )/ $C_{60}$ ( $300 \text{ \AA}$ )/BCP( $80 \text{ \AA}$ )/Al( $1000 \text{ \AA}$ ). (b) Dark current (dash dot line) and photocurrent (solid line) density–voltage ( $I$ - $V$ ) curves of the photovoltaic device with the same structure after 30 min heat treatment at  $100 \text{ }^\circ\text{C}$  in a glove box under nitrogen environment. The inset diagram shows the calculation of the series resistance ( $R_s$ ) of the heated device from the linear part of the dark curve.

Figure 2 shows the UV-vis spectra of untreated tetracene film and tetracene film after 30 min heat treatment at  $100 \text{ }^\circ\text{C}$  in a glove box under nitrogen environment. There is almost no difference between the two spectra, indicating no chemical reaction during the heat treatment. Therefore, the differ-

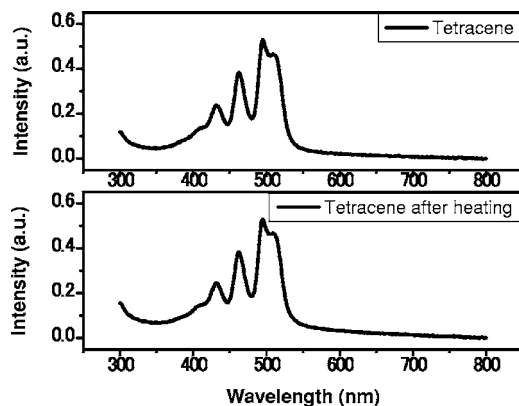


FIG. 2. UV-vis spectra of untreated tetracene film and tetracene film after 30 min heat treatment at  $100 \text{ }^\circ\text{C}$  in a glove box under nitrogen environment.

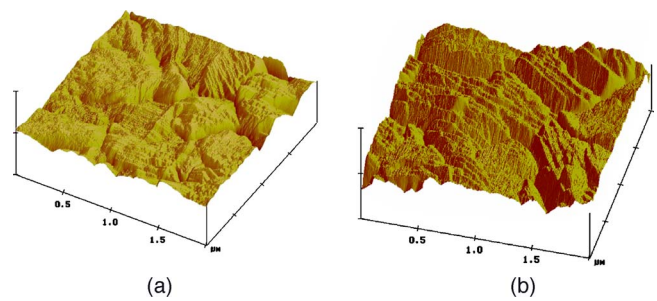


FIG. 3. (Color online) (a) Atomic force microscope (AFM) image of untreated tetracene film. (b) AFM image of tetracene film after 30 min heat treatment at  $100 \text{ }^\circ\text{C}$  in a glove box under nitrogen environment.

ence of the photovoltaic devices can only be understood by considering physical changes. Figure 3(a) shows the atomic force microscope (AFM) image of untreated tetracene film with a thickness of about  $1000 \text{ \AA}$ . Figure 3(b) is the AFM image of the same tetracene film after 30 min heat treatment at  $100 \text{ }^\circ\text{C}$  in a glove box under nitrogen environment. The root-mean-square roughnesses for these two films are 7.6 and 9.8 nm, respectively, and the grain sizes are almost the same. It can be observed from the two images that the heat treated tetracene film has become more ordered and some texture of the grains emerge all in roughly one similar direction. This morphology change is suspected to result in higher mobility in tetracene and better device performance. To further testify this assumption, hole only devices were prepared with

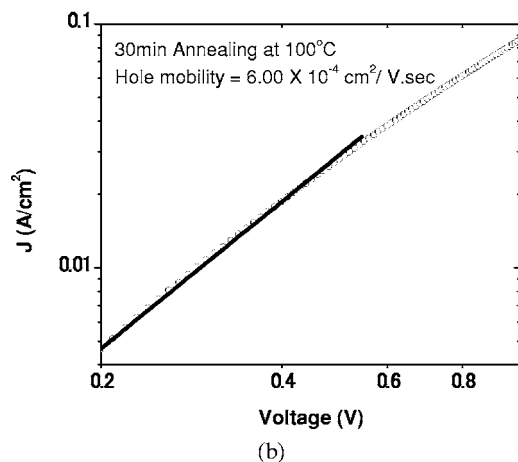
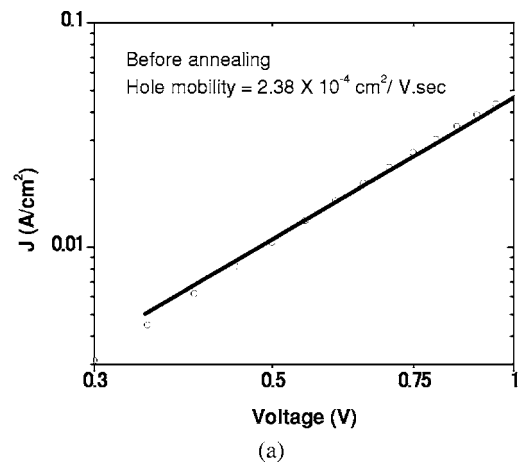


FIG. 4. Dark  $I$ - $V$  curve for hole only device (a) before heat treatment and (b) after heat treatment. The dark line is the fit to the experimental data using SCLC model.

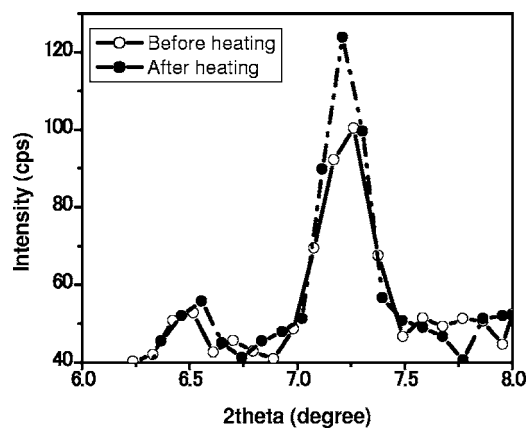


FIG. 5. X-ray diffraction analysis of 180 nm tetracene films on glass substrate before and after heat treatment.

the device structure ITO/PEDOT:PSS/tetracene (800 Å)/molybdenum oxide (MoO<sub>3</sub>) (50 Å)/Al (800 Å).<sup>17</sup> Hole mobilities before and after heat treatment were measured from the dark current density–voltage (*I*-*V*) characteristics of hole only devices. The dark *I*-*V* characteristics before and after heat treatment are shown in Figs. 4(a) and 4(b), respectively. The hole mobility was calculated considering the space charge limited current (SCLC) regime of the *I*-*V* curve according to  $J=9\epsilon_0\epsilon_r\mu V^2/8L^3$ . We observe that the hole mobility increases by over two times from  $2.38 \times 10^{-4}$  to  $6.00 \times 10^{-4}$  cm<sup>2</sup>/V s, when the device is heat treated at 100 °C for 30 min. The hole mobility increases due to ordering in the structure of tetracene film.

This ordered structure could also be confirmed by x-ray diffraction (XRD) analysis. Figure 5 shows the XRD signal intensity change of the 180 nm tetracene films on glass substrate before and after heat treatment. The (001) peak around 7.2° clearly reveals the crystallization phenomena of tetracene films, which was further enhanced by heat treatment.

The effects of heat treatment have also been observed before in other organic photovoltaic systems.<sup>5,10,18,19</sup> There are several shared characteristics for these different organic photovoltaic devices, such as higher *V*<sub>OC</sub> and better energy conversion efficiencies. On the other hand, different material systems also show their particular properties. In the process of formation of a bulk heterojunction,<sup>18</sup> the donor CuPc and acceptor 3,4,9,10-perylene tetracarboxylic bis-benzimidazole both undergo morphological changes and phase segregation at the same time. For pentacene/C<sub>60</sub> and tetracene/C<sub>60</sub> heterojunction structures, pentacene and tetracene tend to undergo greater morphological transformation than C<sub>60</sub> since their thermal stabilities are not as high as C<sub>60</sub>. The previously reported pentacene/C<sub>60</sub> device showed improvement of the rectification<sup>10</sup> after heat treatment and smaller dark currents were observed under reverse bias. In our tetracene/C<sub>60</sub>

device, however, opposite results are found. The current density in the dark at –2 V increases from  $-7.2 \times 10^{-3}$  to  $-1.2 \times 10^{-2}$  mA/cm<sup>2</sup> after 30 min heat treatment at 100 °C, and longer heat treatments might result in larger leakage current and worse device performance. This increment in dark current under reverse bias has also been observed in P3HT:PCBM system upon thermal annealing.<sup>20</sup>

In conclusion, proper heat treatment for a tetracene/C<sub>60</sub> heterojunction photovoltaic device can improve the device performance by enhancing the open circuit voltage and improving the fill factor. Consequently, the power conversion efficiency has been improved from 1.7% to 2.2%. The preliminary conclusion for this enhancement is discussed here and supported by UV-vis spectra, atomic force microscopy images, hole mobility data, and x-ray diffraction analysis.

The authors are indebted to the financial support from the Office of Naval Research (Grant No. N00014-01-1-0136, Program Manager: Paul Armistead).

<sup>1</sup>C. W. Tang, Appl. Phys. Lett. **48**, 183 (1986).

<sup>2</sup>H. Spanggaard and F. C. Krebs, Sol. Energy Mater. Sol. Cells **83**, 125 (2004).

<sup>3</sup>P. Peumans, A. Yakimov, and S. R. Forrest, J. Appl. Phys. **93**, 3693 (2003).

<sup>4</sup>G. Li, V. Shrotriya, J. Huang, Y. Yao, T. Moriarty, K. Emery, and Y. Yang, Nat. Mater. **4**, 864 (2005).

<sup>5</sup>F. Padinger, R. S. Rittberger, and N. S. Sariciftci, Adv. Funct. Mater. **13**, 85 (2003).

<sup>6</sup>J. Xue, S. Uchida, B. P. Rand, and S. R. Forrest, Appl. Phys. Lett. **84**, 3031 (2004).

<sup>7</sup>P. Peumans and S. R. Forrest, Appl. Phys. Lett. **79**, 126 (2001).

<sup>8</sup>G. Yu, J. Gao, J. C. Hummelen, F. Wudl, and A. J. Heeger, Science **270**, 1789 (1995).

<sup>9</sup>S. Yoo, B. Domercq, and B. Kippelen, Appl. Phys. Lett. **85**, 5427 (2004).

<sup>10</sup>A. C. Mayer, M. T. Lloyd, D. J. Herman, T. G. Kasen, and G. G. Malliaras, Appl. Phys. Lett. **85**, 6272 (2004).

<sup>11</sup>C.-W. Chu, Y. Shao, V. Shrotriya, and Y. Yang, Appl. Phys. Lett. **86**, 243506 (2005).

<sup>12</sup>R. W. I. de Boer, A. F. Morpurgo, and T. M. Klapwijk, Appl. Phys. Lett. **83**, 4345 (2003).

<sup>13</sup>F. Cicoira, C. Santato, F. Dinelli, M. Murgia, M. A. Loi, F. Biscarini, R. Zamboni, P. Heremans, and M. Muccini, Adv. Funct. Mater. **15**, 375 (2005).

<sup>14</sup>H. Moon, R. Zeis, E.-J. Borkent, C. Besnard, A. J. Lovinger, T. Siegrist, C. Kloc, and Z. Bao, J. Am. Chem. Soc. **126**, 15322 (2004).

<sup>15</sup>C. Santato, I. Manunza, A. Bonfiglio, F. Cicoira, P. Cosseddu, R. Zamboni, and M. Muccini, Appl. Phys. Lett. **86**, 141106 (2005).

<sup>16</sup>V. Shrotriya, G. Li, Y. Yao, T. Moriarty, K. Emery, and Y. Yang, Adv. Funct. Mater. **16**, 2016 (2006).

<sup>17</sup>V. Shrotriya, Y. Yao, G. Li, and Y. Yang, Appl. Phys. Lett. **89**, 063505 (2006).

<sup>18</sup>P. Peumans, S. Uchida, and S. R. Forrest, Nature (London) **425**, 158 (2003).

<sup>19</sup>M. Al-Ibrahima, O. Ambacher, S. Sensfuss, and G. Gobsch, Appl. Phys. Lett. **86**, 201120 (2005).

<sup>20</sup>G. Li, V. Shrotriya, Y. Yao, and Y. Yang, J. Appl. Phys. **98**, 043704 (2005).